Experimental Evaluation of Basic Circuit Components Using Buried Microstrip Lines for Constructing High-Density Microwave Integrated Circuits

Takahide Ishikawa, *Member, IEEE*, and Eikichi Yamashita, *Fellow, IEEE*

***Abstract*— The buried microstrip line (BMSL) is a promising transmission line structure for realizing low crosstalk characteristics. The measured crosstalk characteristics of model BMSL's have shown good agreement with the estimated ones based on the rectangular boundary division method and the finite-difference time-domain (FDTD) method, indicating that these calculation methods are appropriate for estimating the performance of BMSL's. These results also confirm our expectation that BMSL's have extremely low crosstalk characteristics such as −100 dB in real circuits at high microwave frequencies. The basic circuit components to construct high-density microwave circuits using BMSL's, couplers, stub matching circuits, and gap-coupled resonance filter circuits, were fabricated and experimentally evaluated.**

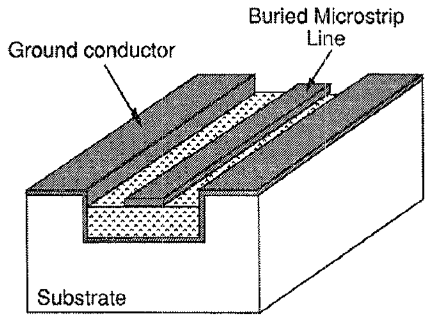

Fig. 1. Buried microstrip line (BMSL) which consists of a buried dielectric material, a strip conductor, and a ground conductor layer surrounding the buried dielectric material.

I. Introduction

High isolation or low crosstalk transmission lines are of the foremost importance in realizing high-density microwave integrated circuits because the high density of microwave integrated circuits (MIC's) and monolithic microwave/millimeter wave integrated circuits (MMIC's) forces us to make distances between interconnects in MIC's and MMIC's extremely short and such short distances can lead to serious crosstalk in such circuits. With the increasing demands for downsized MIC's and MMIC's especially those for hand-held microwave devices such as cellular phones, the study of high isolation transmission lines is becoming much more significant. Although several papers have been published in the past on reducing the coupling between two closely placed lines [1], [2], guided wave structures with satisfactorily low crosstalk and with sufficient applicability to MIC's or MMIC's have not yet been reported.

The buried microstrip line (BMSL) shown in Fig. 1 has the potential to the above low cross-talk requirement, and whose structure consists of a dielectric medium through which electromagnetic waves can propagate buried in the substrate of an MIC or MMIC, a strip conductor placed on the top of the buried dielectric, and a ground conductor layer formed to surround the buried dielectric. A BMSL can be formed in any type of supporting substrate including conductive materials, because the electromagnetic waves are transmitted in the buried dielectric. This feature enables us to improve the performances of silicon MMIC's by reducing the loss in transmission lines. The same structure has been studied in the case of a single transmission line by Rozzi *et al.* [3]–[5]. To our knowledge, however, the crosstalk characterization of this structure for application in high-density microwave integrated circuits has not yet been reported.

In our previous paper [6], the BMSL was characterized using the rectangular boundary division (RBD) method [7]–[9] based on the quasi-TEM wave approximation and the finite-difference time-domain (FDTD) method [10]. It was clarified for the first time that BMSL's possess much lower crosstalk characteristics than conventional microstrip lines, such as −100 dB, and are suited to high-density microwave integrated circuits. It was also revealed that the quasi-TEM wave approximation is applicable to designing the circuits with BMSL's, because the results calculated by the RBD method showed good agreement with those by the FDTD method. Next, BMSL stub circuits, which are essential for constructing matching networks for microwave integrated circuits, were analyzed by the FDTD method and the feasibility of the matching networks was demonstrated.

In this paper, we describe the fabrication and measured data of BMSL circuits to confirm the validity of the simulation results in [6]. Several types of BMSL circuits were constructed, namely, couplers for the evaluation of crosstalk characteristics,

Manuscript received August 28, 1995; revised March 20, 1996.
T. Ishikawa is with the Optoelectronic and Microwave Devices Laboratory, Mitsubishi Electric Corporation, 4-1 Mizuhara, Itami, Hyogo 664, Japan.
E. Yamashita is with the Department of Electronic Engineering, University of Electro-Communications, 1-5-1 Chofugaoka, Chofu-shi, Tokyo 182, Japan.
Publisher Item Identifier S 0018-9480(96)04708-4.

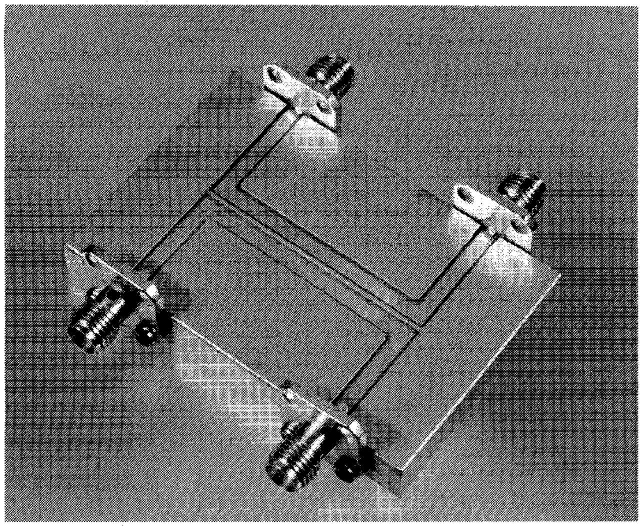

Fig. 2. Photograph of a BMSL coupler for evaluation of crosstalk characteristics of BMSL's. Gold-plated covar is used for the substrate material and polyimide ($\varepsilon_r = 3.4$) is used for the buried dielectric.

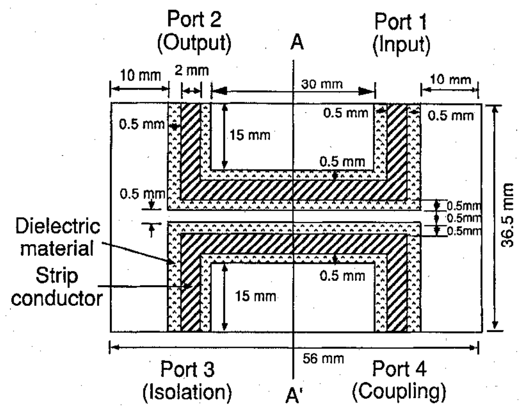

Fig. 3. Top view and dimensions of fabricated couplers. Two types of couplers were fabricated and they have identical dimensions for the top surface as shown here.

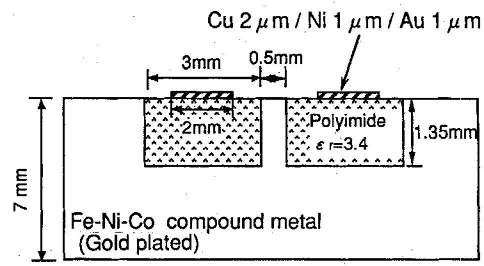

Fig. 4. Cross-sectional view at A-A′ in Fig. 3 for a coupler with a buried depth of $d = 0$ mm. It has a designed coupling coefficient of −30.8 dB. The characteristic impedance of the line is 50 Ω.

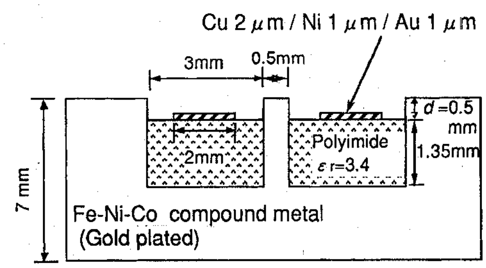

Fig. 5. Cross-sectional view at A-A′ in Fig. 3 for a coupler with a buried depth of $d = 0.5$ mm. It has a designed coupling coefficient of −39.0 dB. The characteristic impedance of the line is 47 Ω.

stub circuits for the confirmation of the feasibility of matching networks, and a gap-coupled resonance filter circuit for the evaluation of resonance performances.

II. Fabrication and Evaluation of BMSL Circuit Components

A. BMSL Couplers

The BMSL couplers shown in Fig. 2 were fabricated in order to confirm their low crosstalk characteristics. Gold-plated covar was used as the supporting material and polyimide ($\varepsilon_r = 3.4$) was used as the buried dielectric material. The 3 mm wide grooves in the BMSL's were formed by digging the substrate with an NC machine. Then 1.35 mm thick, 3 mm wide polyimide was placed in the covar grooves. Conductor strip lines of 2 mm wide Cu 2 μm/Ni 1 μm/Au 1 μm were deposited on the top of the polymide by the selective plating technique. Fig. 3 shows a top view and the dimensions of the fabricated BMSL coupler. Two types of the BMSL couplers with different cross-sectional dimensions were constructed. These cross-sectional views of the two couplers at A-A′ in Fig. 3 are shown in Figs. 4 and 5. The first one shown in Fig. 4 has a buried depth, d, of 0 mm with a designed coupling level of −30.8 dB. The second one shown in Fig. 5 has a buried depth of 0.5 mm with a designed coupling coefficient of −39.0 dB. The characteristic impedance of the lines in Fig. 4 is 50 ohms and that of the lines in Fig. 5, 47 ohms. The dimensions at the top surface of the two BMSL couplers are identical.

Various S-parameters were measured to evaluate the crosstalk characteristics of the BMSL's. The measurement was carried out for the isolation port ($|S_{31}|$) and coupling port ($|S_{41}|$) by using a network analyzer, HP8510B. Numerical analyzes were also conducted to compare the measured results with the calculated ones. As in the previous paper [6], two types of design methods were employed, namely, the RBD and FDTD methods. The S-parameters were calculated using the formulae by Yamamoto *et al.* [11] and using the quasi-TEM parameters calculated by the RBD method. In the FDTD analysis, a Gaussian pulse is injected into Port 1 whose waveform is given by

$$E_x(t\Delta t) = \exp\left(-\frac{(t-t_0)^2}{T^2}\right). \tag{1}$$

The values of t_0 and T are set as 270 steps and 90 steps, respectively. These parameters give the maximum analysis frequency of 20 GHz. The cell dimensions are $\Delta x = 0.5$ mm, $\Delta y = 0.25$ mm, and $\Delta z = 0.25$ mm for the BMSL coupler as shown in Fig. 4, and $\Delta x = 0.27$ mm, $\Delta y = 0.25$ mm, and $\Delta z = 0.25$ mm for the BMSL coupler shown in Fig. 5. The time step duration is $\Delta t = 0.4$ ps for both cases, which are

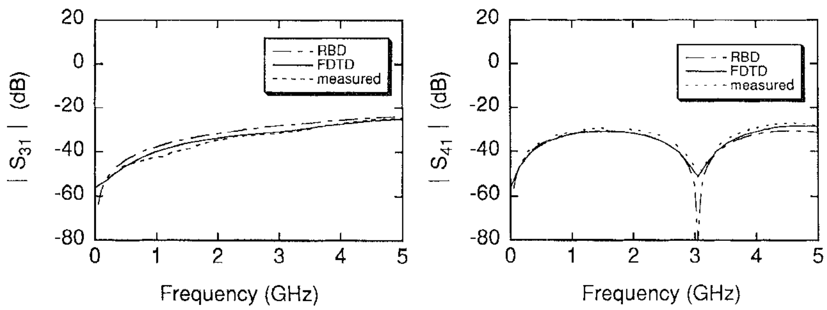

(a) (b)

Fig. 6. Crosstalk characteristics of a coupler of a buried depth of $d = 0$ mm. Experimental and calculated results show good agreement, indicating that the calculation procedures we have employed and their calculated results are valid. Also, quasi-TEM approximation is valid for the BMSL structure. (a) S-parameters observed at the isolation port ($|S_{31}|$). (b) S-parameters observed at the isolation port ($|S_{41}|$).

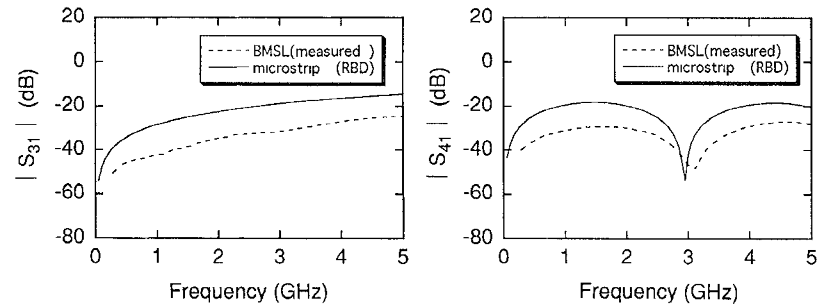

(a) (b)

Fig. 7. Comparison of crosstalk characteristics between BMSL's and conventional microstrip lines with the same dimensions as in the coupler of $d = 0.5$ mm BMSL's have an about 20 dB lower crosstalk level than microstrip lines for this case. (a) Results for $|S_{31}|$. (b) Results for $|S_{41}|$.

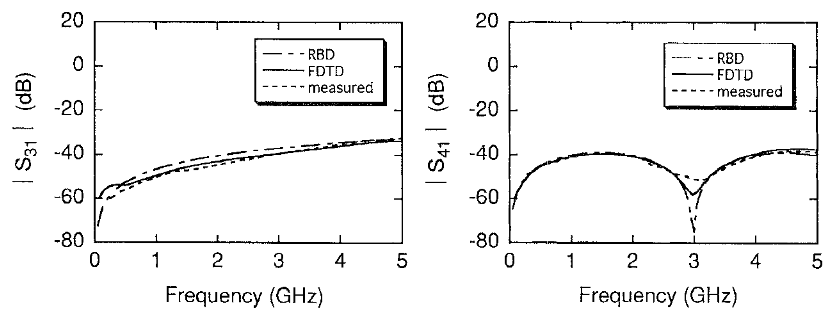

(a) (b)

Fig. 8. Crosstalk characteristics of a coupler with a buried depth of 0.5 mm. Experimental and calculated results show good agreement, indicating that the calculation procedures we employed and their calculated results are valid. Also, the quasi-TEM approximation is valid for the BMSL structure. (a) S-parameters observed at the isolation port ($|S_{31}|$). (b) S-parameters observed at the isolation port ($|S_{41}|$).

derived from the Courant condition [12] given as

$$v\Delta t \le \frac{1}{\sqrt{\frac{1}{(\Delta x)^2} + \frac{1}{(\Delta y)^2} + \frac{1}{(\Delta z)^2}}}. \quad (2)$$

The absorbing boundary conditions adopted for the FDTD analysis are Mur's 1st and 2nd order conditions [13]. The numbers of cells are $n_x = 9, n_y = 174$, and $n_z = 178$ for the BMSL coupler shown in Fig. 4, and $n_x = 21, n_y = 174$, and $n_z = 178$ for the BMSL coupler shown in Fig. 5.

The measured and calculated values for the BMSL coupler shown in Fig. 4 are plotted in Fig. 6(a) and (b). Fig. 6(a) shows the S-parameters at the isolation port ($|S_{31}|$) and Fig. 6(b) shows those at the coupling port ($|S_{41}|$). In these figures, the measured values and those calculated by the two different analysis methods indicate very good agreement. The measured coupling coefficient at the first local maximum value is -29.4 dB and this value is well consistent with the design value of -30.8 dB of the coupler. A comparison of the crosstalk characteristics of the BMSL's with those of conventional microstrip lines was done to see the low crosstalk effect of BMSL as plotted in Fig. 7(a) and (b). Here, the crosstalk characteristics of the microstrip lines with the BMSL coupler of the same dimensions were estimated by the RBD method. The figures show that BMSL's have about a 10 dB lower crosstalk level than those of microstrip lines. Fig. 8(a) and (b) show the measured and calculated values for the coupler in Fig. 5 where good agreement is observed. The measured coupling coefficient at the first local maximum value of the

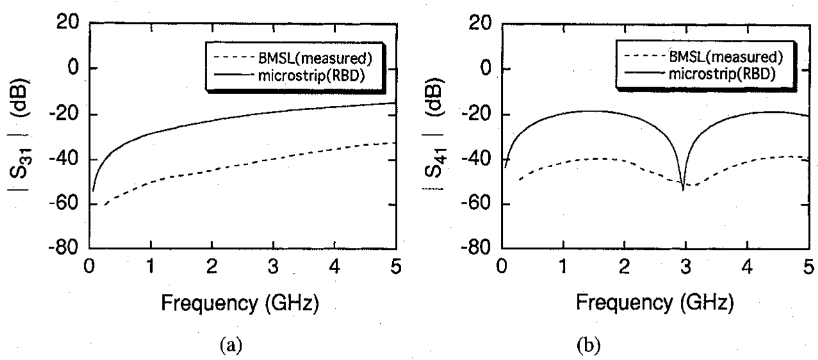

Fig. 9. Comparison of crosstalk characteristics of BMSL's with those of conventional microstrip lines having the same dimensions as in the $d = 0.5$ mm coupler. BMSL's have about 20 dB lower crosstalk than microstrip lines for this case. (a) Results for $|S_{31}|$. (b) Results for $|S_{41}|$.

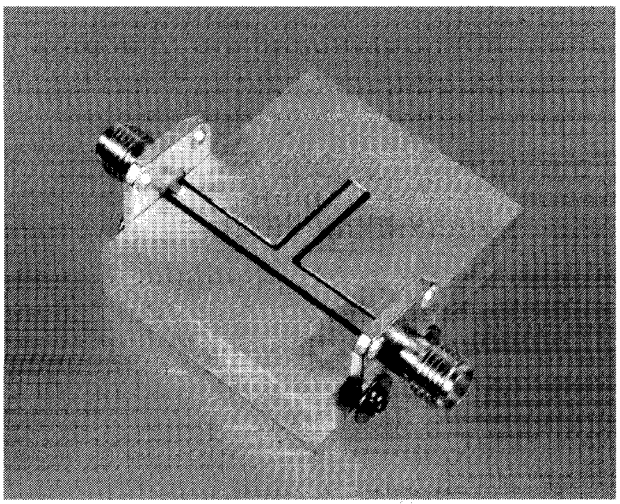

Fig. 10. Photograph of a BMSL short stub circuit to investigate the feasibility of short matching networks, which are essential to realize BMSL microwave integrated circuits.

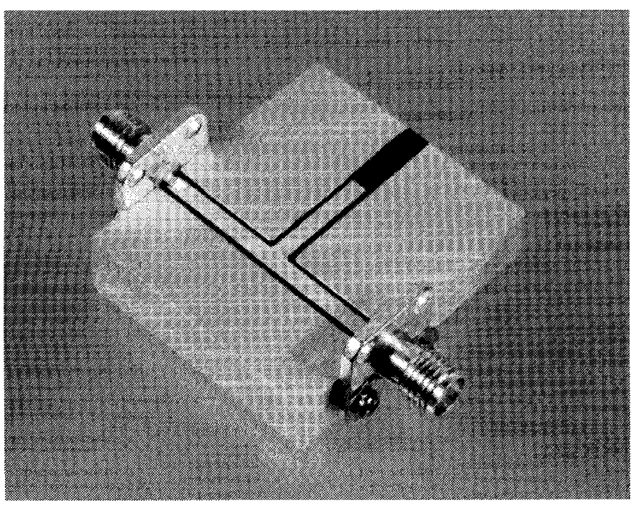

Fig. 11. Photograph of a BMSL open stub circuit to investigate the feasibility of open matching networks, which are essential to realize BMSL microwave integrated circuits.

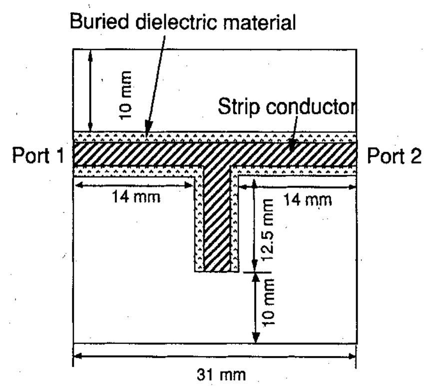

Fig. 12. Top view and the dimensions of a fabricated short stub circuit. The cross-sectional dimensions are identical with the BMSL in Fig. 4.

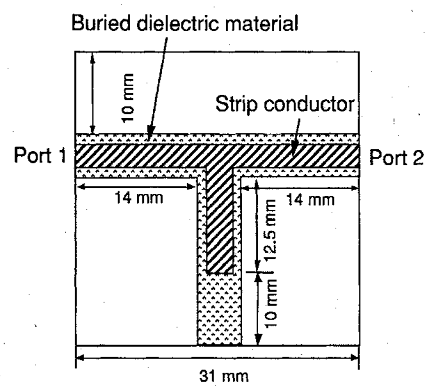

Fig. 13. Top view and the dimensions of a fabricated open stub circuit. The cross-sectional dimensions are identical with the BMSL in Fig. 4.

coupler is −39.5 dB. This value is well consistent with the design value of −39.0 dB. Comparison of the crosstalk of BMSL's and those of conventional microstrip lines was made as plotted in Fig. 9(a) and (b). The figures show that BMSL's have about a 20 dB lower crosstalk level than those of microstrip lines. The results in Figs. 6–9(b) clearly indicate that our numerical analysis methods are appropriate and BMSL's certainly have much lower crosstalk levels than microstrip lines. In these experiments, the line dimensions were set larger than those in MMIC's or MIC's to make the fabrication and testing easy. Good agreement between the quasi-TEM approximation and the experimental results should be maintained in BMSL's in microwave integrated circuits, which have very small dimensions.

In these experiments the burial depth, d, was chosen as 0 mm and the relatively small value of 0.5 mm to obtain rather large coupling coefficients, such as −30 and −40 dB

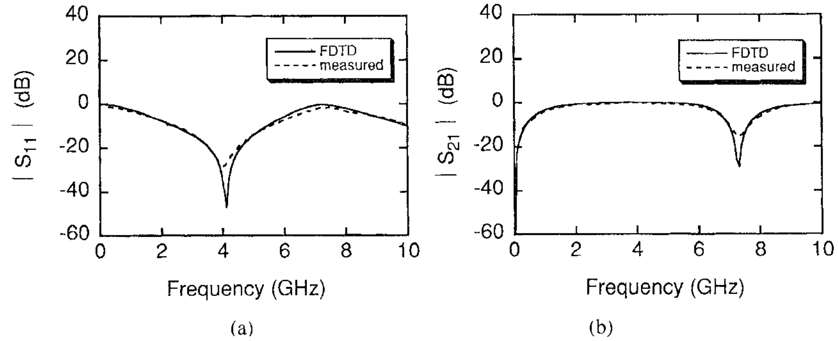

Fig. 14. (a) S-parameters observed at Port 1 of a BMSL short stub circuit ($|S_{11}|$). (b) S-parameters observed at Port 2 of a BMSL short stub circuit ($|S_{21}|$). Measured and calculated results by the FDTD method show good agreement for both ports. Also the results have good agreement with the projected shunt and transmission frequencies calculated by the quasi-TEM approximation.

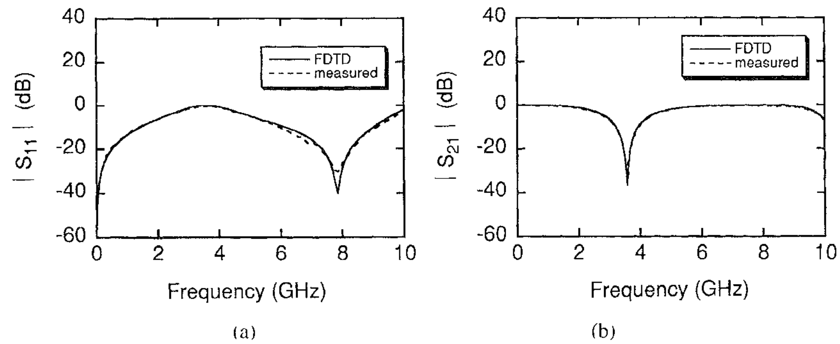

Fig 15. (a) S-parameters observed at Port 1 of a BMSL open stub circuit ($|S_{11}|$). (b) S-parameters observed at Port 2 of a BMSL open stub circuit ($|S_{21}|$). The measured results and the results calculated by the FDTD method show good agreement for both the ports. Also the results have good agreement with the projected shunt and transmission frequencies calculated by the quasi-TEM approximation.

considering the limitations of measurements. The extremely low crosstalk level of -100 dB as described in the previous paper [6] was not directly measured in this work. However, the present agreement between the calculated and measured values of the BMSL couplers enables us to confirm that the BMSL has extremely small crosstalk levels.

B. Stub Matching Circuits

A BMSL short stub circuit and open stub circuit, which are essential components to realize BMSL microwave integrated circuits, were fabricated to investigate their performance. Photographs of the short and open stub circuits are shown in Figs. 10 and 11, respectively. Figs. 12 and 13 show the top views and the dimensions of the short and open stub circuits, respectively. The stub length was 12.5 mm in both cases. The cross-sectional dimensions of the BMSL's are the same as the BMSL's in Fig. 4. Fig. 14(a) and (b) show $|S_{11}|$ and $|S_{21}|$ of the short stub circuit while Fig. 15(a) and (b) show $|S_{11}|$ and $|S_{21}|$ of the open stub circuit. These measured values are compared with the simulation results by the FDTD method where the same discretion parameters as in the case of the BMSL coupler as shown in Fig. 4 are used. The cell numbers are as $n_x = 9, n_y = 492$, and $n_z = 92$. Good agreement between the measured values and the ones calculated by the FDTD analysis is found in all four of the figures. The shunt and transmission frequencies of the stub circuits are estimated by the following formula with the quasi-TEM approximation.

$$\lambda = \frac{v_0}{f} \Big/ \sqrt{\varepsilon_{\text{eff}}} \tag{3}$$

where v_0 is the velocity of light in a vacuum, f is the frequency, and ε_{eff} is the effective dielectric constant.

The value of ε_{eff} is calculated as 2.41 by the RBD method. The transmission frequency f_{ts} of the short stub is given as

$$f_{\text{ts}} = 3.87 \times (2n - 1) \quad \text{(GHz)} \quad (n = 1, 2, 3, \ldots) \tag{4}$$

the shunt frequency, f_{ss}, of the short stub is

$$f_{\text{ss}} = 3.87 \times 2n \quad \text{(GHz)} \quad (n = 1, 2, 3, \ldots) \tag{5}$$

the transmission frequency, f_{to}, of the open stub is

$$f_{\text{to}} = 3.87 \times 2n \quad \text{(GHz)} \quad (n = 1, 2, 3, \ldots) \tag{6}$$

and the shunt frequency, f_{so}, of the open stub is

$$f_{\text{so}} = 3.87 \times (2n - 1) \quad \text{(GHz)} \quad (n = 1, 2, 3, \ldots). \tag{7}$$

In Figs. 14 and 15, the values estimated by these formulae show good agreement with the measured values, indicating that the short and open stubs matching circuits can be readily realized for BMSL microwave integrated circuits. The slight difference seen between the projected shunt and transmission frequencies and the measured values in the figures is due to parasitic inductance in the short stub and parasitic capacitance in the open stup circuit.

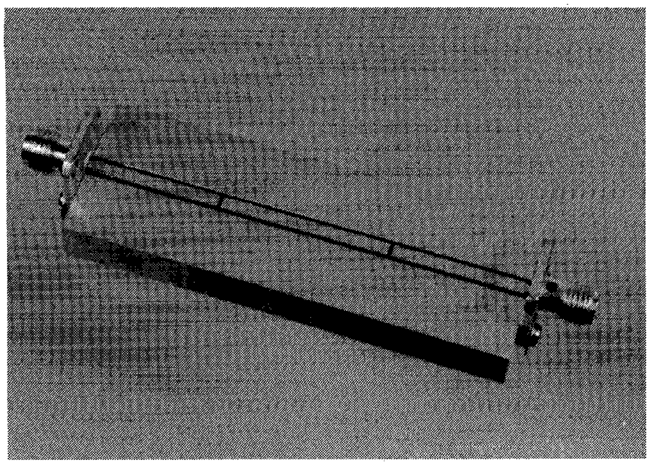

Fig. 16. Photograph of a BMSL gap resonance filter circuit to investigate a BMSL circuit with discontinuities.

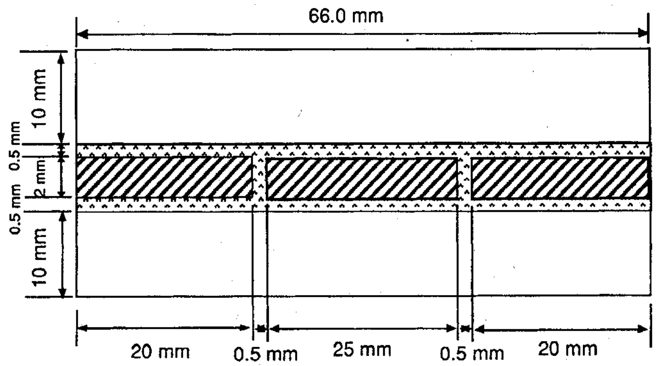

Fig. 17. Top view and the dimensions for a gap-coupled resonance filter circuit of BMSL. The cross-sectional view and the dimensions are the same as the one in Fig. 4.

C. Gap-Coupled Resonance Filter Circuit

A BMSL gap-coupled resonance filter circuit as another BMSL circuit component is shown in Fig. 16. A top view and the dimensions of the circuit are shown in Fig. 17. Two gaps are formed along a BMSL strip conductor. The gap length is 0.5 mm and the distance between the two gaps is 25 mm. The cross-sectional dimensions of the BMSL for this circuit are the same as those in Fig. 4. The experimental data and those calculated by the FDTD method are depicted in Fig. 18 where the same discretion parameters as in the coupler in Fig. 4 were used. The numbers of the cells for the FDTD analysis are $n_x = 9, n_y = 492$, and $n_z = 92$. The experimental and measured $|S_{11}|$ values show good agreement while a small difference is seen for $|S_{21}|$. This is perhaps because the FDTD simulation underestimates the radiation loss in the circuit. The resonance frequencies of the filter are estimated by the following formula with the quasi-TEM approximation

$$f_r = 3.87 \times n \quad \text{(GHz)} \quad (n = 1, 2, 3, \ldots). \qquad (8)$$

The measured resonance frequencies are consistent with the values estimated by the formula (8), indicating that BMSL gap-coupled resonance filter circuits perform in a similar fashion to their microstrip line counterparts.

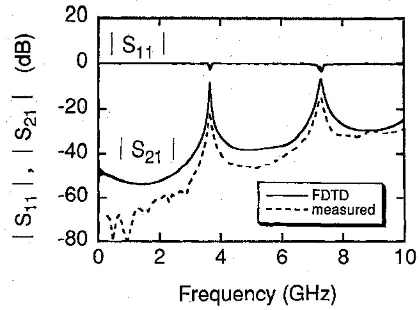

Fig. 18. Measured S-parameters at Port 1 ($|S_{11}|$) and Port 2 ($|S_{21}|$) for a BMSL gap resonance filter circuit. They show fairly good agreement with the results calculated by the FDTD method. Also they have good agreement with the projected resonance frequencies calculated on the basis of the quasi-TEM approximation.

III. Conclusion

BMSL couplers, stub matching circuits, and gap-coupled resonance filter circuits were fabricated as basic circuit components for constructing high-density microwave circuits and were experimentally evaluated.

The BMSL couplers were fabricated to measure their crosstalk levels. Good agreement between the experimental values and those calculated by the RBD and FDTD methods confirmed our previous expectation that BMSL's possess extremely low crosstalk levels, such as -100 dB.

BMSL stub matching circuits, which are essential when BMSL's are incorporated in microwave integrated circuits, were also fabricated and evaluated by measuring the S-parameters. The BMSL short and open stub circuits demonstrated the performances predicted by the FDTD and RBD methods. The fact that BMSL's can easily provide matching networks clearly indicates that the BMSL structure is quite practical for constructing microwave integrated circuits.

The performance of the fabricated BMSL gap-coupled resonance filter circuit showed fairly good agreement with the performance calculated by the FDTD and RBD methods. This indicates that BMSL is not only a high isolation transmission line but it has the great advantage that it can offer the same type of microwave circuit components as conventional microstrip lines do.

In conclusion, BMSL is a promising transmission line structure for constructing microwave integrated circuits.

Acknowledgment

The authors would like to thank N. Kishi, Y. Qian, and H. Kirino of the University of Electro-Communications for their helpful discussions throughout this work. They would like to express their gratitude to O. Ishihara, M. Otsubo, H. Takano, N. Tanino, and H. Oh-hashi of Mitsubishi Electric Corporation for their continuous support.

References

[1] S. He, A. Z. Elsherbeni, and C. Smith, "Decoupling between two conductor microstrip transmission lines," *IEEE Trans. Microwave Theory Tech.*, vol. 41, no. 1, pp. 53–61, Jan. 1993.

[2] N. G. Alexopoulos and C. M. Krowne, "Characteristics of single and coupled microstrips on anisotropic substrates," *IEEE Trans. Microwave Theory Tech.*, vol. 26, no. 6, pp. 387–393, June 1978.

[3] T. Rozzi, A. Morini, and G. Gerini, "Analysis and applications of microstrip-loaded inset dielectric waveguide (Mig)," *IEEE Trans. Microwave Theory Tech.*, vol. 40, no. 2, pp. 272–278, Feb. 1992.

[4] N. Izzat, S. R. Pennock, and T. Rozzi, "Space domain analysis of micro-IDG structures," *IEEE Trans. Microwave Theory Tech.*, vol. 42, no. 6, pp. 1074–1078, June 1994.

[5] T. Rozzi, G. Gerini, A. Morini, and M. De Santis, "Multilayer buried microstrip inset guide," *European Microwave Conf. Dig.*, 1991, pp. 673–678.

[6] T. Ishikawa and E. Yamashita, "Low crosstalk characteristics of buried microstrip lines," *1995 MTT-S Int. Microwave Symp. Dig.*, 1995, pp. 853–856.

[7] E. Yamashita, M. Nakajima, and K. Atsuki, "Analysis method for generalized suspended striplines," *IEEE Trans. Microwave Theory Tech.*, vol. 34, no. 12, pp. 1457–1463, Dec. 1986.

[8] H. Takasu and E. Yamashita, "Impedance characterization of GaAs FET switches," *IEEE Trans. Microwave Theory Tech.*, vol. 40, no. 7, pp. 1422–1429, July 1992.

[9] E. Yamashita, K. R. Li, and Y. Suzuki, "Characterization method and simple design formulas of MCS lines proposed for MMIC's," *IEEE Trans. Microwave Theory Tech.*, vol. 35, no. 12, pp. 1355–1362, Dec. 1987.

[10] K. S. Yee, "Numerical solution of initial boundary value problems involving Maxwell's equations in isotropic media," *IEEE Trans. Antennas Propagat.*, vol. AP-14, pp. 302–307, May 1966.

[11] S. Yamamoto, T. Azakami, and K. Itakura, "Coupled nonuniform transmission line and its applications," *IEEE Trans. Microwave Theory Tech.*, vol. 15, no. 4, pp. 220–231, Apr. 1967.

[12] A. Taflove and M. E. Brodwin, "Numerical solution of steady-state electromagnetic scattering problems using the time-dependent Maxwell's equations," *IEEE Trans. Microwave Theory Tech.*, vol. 23, pp. 623–630, 1975.

[13] G. Mur, "Absorbing boundary condition for the finite-difference approximation of the time-domain electromagnetic-field equations," *IEEE Trans. Electromag. Compat.*, vol. 23, no. 4, pp. 377–382, 1981.

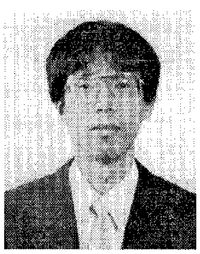

Takahide Ishikawa (M'95) was born in Kagawa, Japan, on July 2, 1958. He received the B.S., M.S., and Ph.D. degrees in electronic engineering from the University of Electro-Communications, Tokyo, Japan, in 1981, 1983, and 1996, respectively.

In 1983 he joined the LSI Research and Development Laboratory, Mitsubishi Electric Corporation, Hyogo, Japan. Since then he has been engaged in the development of GaAs MMIC process and device technologies especially in FET amplifiers for low-noise and high power applications. He is currently an Assistant Manager in the GaAs IC Engineering Group, Microwave Devices Development Department, Optoelectronic and Microwave Devices Laboratory, Hyogo, Japan. His research interests include numerical analyzes and experiments on microwave and millimeter-wave circuits.

Dr. Ishikawa is a member of the Institute of Electronics, Information, and Communication Engineers of Japan.

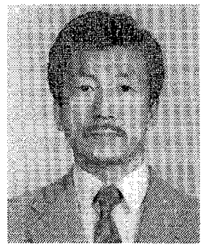

Eikichi Yamashita (M'66–SM'79–F'84) was born in Tokyo, Japan, on February 4, 1933. He received the B.S. degree from the University of Electro-Communications, Tokyo, Japan, and the M.S. and Ph.D. degrees from the University of Illinois, Urbana, IL, USA, all in electrical engineering, in 1956, 1963, and 1966, respectively.

From 1956 to 1964, he was a Member of the research staff on millimeter-wave engineering at the Electrotechnical Laboratory, Tokyo, Japan. While on leave from 1961 to 1963 and from 1964 to 1966, he studied solid-state devices in the millimeter-wave region at the the Electro-Physics Laboratory, University of Illinois. He became Associate Professor in 1967 and Professor in 1977 in the Department of Electronic Engineering, Dean of Graduate School from 1992 to 1994, the University of Electro-Communications, Tokyo, Japan. His research work since 1956 has been principally on applications of electromagnetic waves such as various microstrip transmission lines, wave propagation in gaseous plasma, pyroelectric-effect detectors in the submillimeter-wave region, tunnel-diode oscillators, wide-band laser modulators, various types of optical fibers, ultra-short electrical pulse propagation on transmission lines, and millimeter-wave imaging. He is editor of *Analysis Methods for Electromagnetic Wave Problems (vol. 1 and vol. 2),* (Norwood, MA: Artech).

Dr. Yamashita was Chairperson of the Technical Group on Microwaves, IEICE, Japan, from 1985 to 1986, and Vice-Chairperson, Steering Committee, Electronics Group, IEICE, from 1989 to 1990. He served as Associate Editor of the IEEE TRANSACTIONS ON MICROWAVE THEORY AND TECHNIQUES from 1980 to 1984. He was elected Chairperson of the MTT-S Tokyo Chapter from 1985 to 1986. He has been a member of the MTT-S ADCOM since January 1992, and Chairperson of Chapter Operations Committee, IEEE Tokyo Section since 1995. He served as Chairperson of International Steering Committee, 1990 and 1994 Asia-Pacific Microwave Conference, held in Tokyo and sponsored by the IEICE.